Ellis, S. R. M., University of Birmingham, UK, Private communication (1972).
Fair, J. R., "Design of Equilibrium Stage Processes," by B. D. Smith, p. 551, McGraw-Hill, New York (1963).
Foss, A. S., and J. A. Gerster, "Liquid Film Efficiencies on Sieve Trays," *Chem. Eng. Progr.*, **52**, 28-J (1956).
Hinze, J. O., "Oscillations of a Gas/Liquid Mixture on a Sieve Plate," Symp. on Two-Phase Flow, F-101, University of Exeter, UK (1965).
Hunt, C. d'A., D. N. Hanson, and C. R. Wilke, "Capacity Factors in the Performance of Perforated Plate Columns," *AIChE J.*, **1**, 441 (1955).
Leva, M., "Film Tray Equipment for Vacuum Distillation," *Chem. Eng. Progr.*, **67**(3), 65 (1971).
Ludwig, E. E., "Applied Process Design for Chemical and Petrochemical Plants," Vol. II, p. 98, Gulf, Houston (1964).
McAllister, R. A., and C. A. Plank, "Pulsations in Sieve-tray and Bubble-cap Distillation Towers," *AIChE J.*, **4**, 283 (1958).
McAllister, R. A., P. H. McGinnis, Jr., and C. A. Plank, "Perforated Plate Performance," *Chem. Eng. Sci.*, **9**, 25 (1958).
Ravicz, A. E., Chevron Research Co., Richmond, California, Private communication (1972).

Manuscript received May 10, 1973; revision received August 28 and accepted September 4, 1973.

Analysis of the Normal Stress Extruder

A theoretical and experimental investigation of the pumping characteristics of the normal stress extruder was made. The theoretical model requires only material property data and extruder dimensions and rotation speed to evaluate the main velocity field, flow rate, and pressure. The flow from the extruder was measured for two viscoelastic polymer solutions and a polymer melt as a function of gap setting and angular velocity. These measurements were in reasonable agreement with the proposed model.

PAUL A. GOOD
ARTHUR J. SCHWARTZ
and
CHRISTOPHER W. MACOSKO

Department of Chemical Engineering and Materials Science
University of Minnesota
Minneapolis, Minnesota 55455

SCOPE

Two important operations in the polymer processing industry are the melting of polymer feed stocks and the mixing of additives, such as plasticizers or coloring agents, with the polymer to give desired properties to the finished products. These operations are usually performed in a screw extruder, which can simultaneously develop the large pressures necessary for later processing steps.

An alternate process to perform these operations is the elastic or normal stress extruder. This device utilizes the normal stresses developed between a rotating and stationary disk to pump polymer melts out the center of one disk. Desirable mixing characteristics of the normal stress extruder have generally been neglected because it does not develop large operating pressures. Blends of incompatible polymers from the normal stress extruder are characterized by a filament structure (Starita, 1972) which contrasts sharply with the granular structure resulting with some other types of mixers (Paul, 1972). This highly oriented mixing enhances the mechanical properties of the product and could possibly help stabilize such drawing operations as filament formation.

Development of the normal stress extruder may have been hampered by lack of an adequate model of its operation. This paper is concerned with obtaining an explicit model for the operation of the normal stress extruder. Experimental measurements of the flow rate from the normal stress extruder are made for several viscoelastic materials to verify the proposed model.

CONCLUSIONS AND SIGNIFICANCE

A model of the normal stress extruder which allows the flow rate and pressure generated in isothermal operation of the extruder to be calculated is developed here. The model is largely analytical with some numerical iteration required to evaluate several integrals. The only inputs required for the model are basic rheological data, shear and normal stresses, and extruder dimensions and rotation speed.

Experiments were performed to measure the extrusion rate of a polyisobutylene solution and a polyacrylamide solution. These are viscoelastic fluids which can be pumped isothermally from the normal stress extruder used in the experiments. Comparison of the experimental extrusion rates and the predicted rates indicate the proposed model is adequate for engineering purposes. The model was also used to analyze the polyethylene melt data of Fritz (1971). Comparison of the experimental and predicted flow rates was not as good as the solution data. Due to shear heating the melt was not extruded isothermally. Work is in progress to extend the proposed

Correspondence concerning this paper should be addressed to C. W. Macosko.

model to nonisothermal situations.

The primary use of the normal stress extruder will probably be as a mixer, as it does not develop large pressures characteristic of a screw extruder. Basic to any study of mixing characteristics is a knowledge of the main velocity distributions expected and consequently the extrusion rate. The major significance of the present work is the development of analytical expressions for the velocity distribution in the normal stress extruder, which then allow evaluation of the mixing properties of the extruder on an analytical basis. Such evaluation is now in progress. In addition, this analysis provides the essential framework for design-scale up, optimization, and power requirements.

The normal stress extruder is unique in the area of extrusion equipment. Instead of developing a pumping action through viscous drag effects as with a screw, the normal stress extruder relies on the normal forces generated in a viscoelastic fluid undergoing shear.

Since its inception by Maxwell and Scalora in 1959, the normal stress extruder has been studied experimentally by several authors. L. L. Blyler, Jr. (1966) has studied the velocity distribution in the extruder, Fritz (1971) the flow rates, pressure, and some temperature distributions, J. M. Starita (1972) the mixing properties of the extruder, B. Maxwell (1970, 1972) has presented rough empirical design equations for the extruder, and Kocherov et al. (1973) have studied certain instabilities developed in the extruder. The intent here is to develop an improved analysis of the normal stress extruder.

ANALYSIS OF THE EXTRUDER

The proposed model accounts for the main flow patterns observed in the extruder. The flow geometry is given in Figure 1. The visualization work of Blyler (1966) and Kocherov et al. indicates the normal stress extruder will operate in a steady laminar regime, where all flows are independent of the azimuthal coordinate, provided the gap thickness is not a function of the radial coordinate and the pressure imposed at the periphery is greater than the pressure imposed at the die exit. This is the configuration chosen for experiment and analysis. When operating, the material to be pumped is introduced around the periphery of the disk. The back plate is driven at a constant angular velocity while the die plate is held fixed. For elastic liquids, the fluid flows from the periphery toward the center of the die disk and out the die-opening.

The method of analysis will be to calculate the pressure developed at the die entrance surface $[z = H;\ 0 \leq r \leq R_D]$ caused by elastic normal forces when there is no radial flow. Next, the pressure drop required to produce a flow rate Q from the periphery of the die disk $[r = R]$ to the die entrance surface of a purely viscous fluid is calculated. The difference of these two pressure potentials would then approximate the actual pressure at the die entrance under radial flow conditions. This implies that the total stress tensor $\mathbf{P}$ for a fluid can be expressed as the sum of the isotropic pressure tensor $p\mathbf{I}$, the viscous stress tensor $\boldsymbol{\tau}$, and the elastic normal stress tensor $\mathbf{N}$.

$$\mathbf{P} = -p\mathbf{I} - \boldsymbol{\tau} + \mathbf{N}$$

Such a separation is strictly valid for viscoelastic materials undergoing only locally steady flows, a reasonable assumption for our case as long as V_r is sufficiently small.

To obtain an analytical model, it will be assumed that

1. Extruder is operating in a steady laminar flow regime at constant temperature T
2. Small gap to flow path ratio $(H/(R - R_D) << 1)$
3. Viscous response of the material extruded may be modeled as a power law fluid

$$\boldsymbol{\tau} = -k(\tfrac{1}{2}\boldsymbol{\Delta}:\boldsymbol{\Delta})^{\frac{1}{2}(n-1)}\boldsymbol{\Delta} \quad (1)$$

4. Elastic response can be modeled from torsional flow data as indicated below.

The pressure drop generated by fluid elasticity available to extrude material from the die is given by

$$\Delta p_{NS} = \int_R^{R_D} \left(\frac{dP_{zz}}{dr}\right) dr$$

P_{zz} may be calculated from a constitutive equation which gives the first and second normal stresses due to elasticity as a function of rate of shear.

Δp_{NS} may also be calculated directly from total normal force data from a parallel plate rheometer (Middleman, 1968), where

$$F = \pi \int_R^0 r^2 \left(\frac{dP_{zz}}{dr}\right) dr \quad (2)$$

For the assumed flow in the rheometer dP_{zz}/dr is only a function of the local rate of shear $\dot{\gamma} = \omega r/H$. Thus if the experimental F curve is fit by a trial function,

$$F = \pi R^2 \sum_{i=1} k_i \,\dot{\gamma}_R^{m_i} \quad (3)$$

then

$$\Delta p_{NS} = \sum_{i=1} k_i \frac{m_i + 3}{R} \int_{R_D}^{R} \dot{\gamma}^{m_i}\, dr \quad (4)$$

Blyler et al. (1968) in their analysis of this same system neglect the pressure drop necessary to produce the radial flow distribution in comparison to the pressure drop through the die. The flow rate under these idealized conditions is

$$Q^n = \Theta[\Delta p_{NS} + \Delta p_E] \quad (5)$$

which gives the flow rate of a power law fluid through a tube as a function of the pressure drop along the length of the tube. They assume that entrance and exit effects are negligible and flow in the tube is fully developed and laminar. If R_D/L is not small, entrance effects may become important and must be accommodated. Also the pressure drop required to produce radial flow can not be neglected. Thus Equation (5) predicts flow rates much larger than are experimentally realizable (Blyler, 1966).

The pressure drop required by the radial flow can be calculated from a knowledge of the radial velocity field.

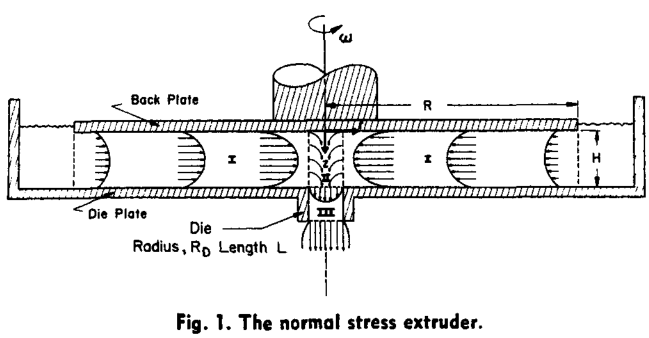

Fig. 1. The normal stress extruder.

The equations governing the velocity field are

$$\frac{1}{r}\frac{\partial}{\partial r}(rV_r) = 0$$

$$\frac{\partial p}{\partial r} = -\left(\frac{1}{r}\frac{\partial}{\partial r}(r(\tau_{rr} - N_{rr})) - \frac{\tau_{\theta\theta} - N_{\theta\theta}}{r} + \frac{\partial \tau_{rz}}{\partial z}\right)$$

$$\frac{\partial p}{\partial z} = -\left(\frac{1}{r}\frac{\partial}{\partial r}(r\,\tau_{rz}) + \frac{\partial}{\partial z}(\tau_{zz} - N_{zz})\right)$$

These equations, with appropriate boundary conditions, could be solved numerically. Fritz (1971) has carried out such calculations after making several a priori simplifications of the equations using rheological relations similar to those used here. His solution is very cumbersome to use in parametric studies and provides little insight into the operation of the extruder. Fritz's results are further obscured by the use of an empirically determined entrance loss number to describe pressure effects in the volume $[0 \leq z \leq H,\ 0 \leq r \leq R_D]$.

For more insight into the normal stress extruder let us consider a quasi-analytical solution which divides the extruder into three regions

Region I: The disk proper
$0 \leq z \leq H$
$R_D \leq r \leq R$

Region II: The die entrance
$0 \leq z \leq H$
$0 \leq r \leq R_D$

Region III: The die proper
$H \leq z \leq L + H$
$0 \leq r \leq R_D$

REGION I: DISK FLOW PROPER

This region may be characterized by the geometrical consideration $H/R << 1$. Because derivatives in the z-direction are much larger than those in the r-direction, a substantial reduction in the equations of motion can be made. The equations describing flow in the disk section are

$$\frac{1}{r}\frac{\partial}{\partial r}(rV_r) = 0 \tag{6}$$

$$\frac{\partial P_{rr}}{\partial r} = \frac{\partial \tau_{rz}}{\partial z} - \frac{\tau_{\theta\theta} - \tau_{rr}}{r} + \frac{N_{\theta\theta} - N_{rr}}{r} \tag{7}$$

Under normal operating conditions

$$\left(\frac{\partial V_\theta}{\partial z}\right)^2 >> 2\left[\left(\frac{\partial V_r}{\partial r}\right)^2 + \left(\frac{V_r}{r}\right)^2\right] + \left(\frac{\partial V_r}{\partial z}\right)^2 \tag{8}$$

and the shear rate can be well approximated by its average defined as

$$\bar{\gamma} = \left(\frac{1}{2H}\int_0^H \mathbf{\Delta}:\mathbf{\Delta}\, dz\right)^{1/2}$$

Consequently, from the power law equation,

$$\frac{dP_{rr}}{dr} = -k\,\bar{\gamma}^{n-1}\frac{\partial^2 V_r}{\partial z^2} + \frac{N_{\theta\theta} - N_{rr}}{r} \tag{9}$$

with boundary conditions

$$V_r(r, 0) = V_r(r, H) = 0 \tag{10}$$

where the normal viscous stresses have been neglected. This is consistent with Equation (6) and is a reasonable assumption if R_D is not too small. As the stress tensor is a linear combination of viscous and normal stress parts, the pressure drop due to viscous stresses and the pressure generated due to normal stresses, Equation (4), may be separated. Equation (9) can be used to calculate the radial velocity and the remaining pressure drop due to viscous flow. The result is

$$V_r = \frac{dp}{dr}\,\frac{z(z-H)}{2k\,\dot{\gamma}^{n-1}} \tag{11}$$

Blyler's tracer studies (1966) support this form for V_r as well as $V_\theta = \omega r(H - z)/H$.

The radial flow in the disk is

$$\begin{aligned} Q &= 2\pi r\int_0^H V_r\, dz \\ &= -\frac{dp}{dr}\,\frac{\pi\, r\, H^3}{6k\,\bar{\gamma}^{n-1}} \end{aligned} \tag{12}$$

The pressure drop due to viscous flow drag in the disk may now be evaluated in terms of the flow rate as

$$\Delta p_{VS} = \frac{6(-Q)}{\pi H^3}\int_{R_D}^{R}\frac{k\bar{\gamma}^{n-1}}{r}\, dr \tag{13}$$

REGION II: DIE ENTRANCE FLOW

Because of the simplified treatment given the radial component of velocity in Region I, one can expect only an equally approximate solution to the die entrance flow problem, since the solution to Region I provides part of the boundary conditions to Region II. The equation of continuity is

$$\frac{1}{r}\frac{\partial}{\partial r}(rU_r) + \frac{\partial}{\partial z}(U_z) = 0 \tag{14}$$

Proposed boundary conditions are

$$U_z = U_r = 0 \qquad z = 0 \quad r \leq R_D \tag{15a}$$

and

$$\left.\begin{aligned} U_z &= \alpha\{1 - [r/R_D]^{(1+n)/n}\} \\ U_r &= 0 \end{aligned}\right\} \qquad z = H \quad r \leq R_D \tag{15b}$$

that is, fully developed power law flow at the die opening, and

$$\left.\begin{aligned} U_z &= 0 \\ U_r &= -\beta z(H - z) \end{aligned}\right\} \qquad 0 \leq z \leq H \quad r = R_D \tag{15c}$$

that, is the proposed flow from region I at $r = R_D$.

Equation (14) may be solved with the boundary conditions (15) to yield

$$\begin{aligned} U_r &= -\Phi r\left[\frac{1}{2} - \frac{n}{1+3n}(r/R_D)^{(1+n)/n}\right] z(H - z) \\ U_\theta &= \frac{\omega r}{H}(H - z) \\ U_z &= \Phi z^2\left[\frac{H}{2} - \frac{z}{3}\right][1 - (r/R_D)^{(1+n)/n}] \end{aligned} \tag{16}$$

The velocity field $\mathbf{U}$ only approximates the actual flow in the die entrance primarily because of the unrealistic pressure boundary conditions imposed on the solution. As treated here, the pressure in disk proper is taken to be only a function of r, and the pressure in the die is taken to be only a function of z. Consequently, there is a pressure discontinuity along the line $[r = R_D,\ z = H]$. As Equation (14) is a first-order equation, one can not specify both the function values and their derivatives on the bounding surface. Consequently, there is also a discontinuity in the rate of shear at the face $(z = H,\ 0 \leq r \leq R_D)$, that is

$$\lim_{z\to H^-} \left(\frac{\partial V_\theta}{\partial z}\right) = -\frac{\omega r}{H} \quad \text{while} \quad \lim_{z\to H^+} \left(\frac{\partial V_\theta}{\partial z}\right) = 0$$

To improve the analysis, the full equations of motion must be solved. To maintain internal consistency, the **U** velocity field was used to evaluate the viscous stresses on the surface and in the volume V for use in Equation (17).

Now that the approximate velocity **U** is known, the pressure drop for flow through Region II can be determined from the mechanical energy balance. For this system, the mechanical energy balance reduces to

$$\int_S \hat{\mathbf{n}} \cdot (p\mathbf{U} + \boldsymbol{\tau} \cdot \mathbf{U})\, dS = \int_V \boldsymbol{\tau} : (\nabla \mathbf{U})\, dV \quad (17)$$

where $\hat{\mathbf{n}}$ is the outward directed normal to the volume V of Region II, and only viscous losses are considered. Equation (17) may be rewritten more explicitly as

$$2\pi R_D \int_0^H [-pU_r + (-\boldsymbol{\tau}\cdot\mathbf{U})_r]|_{r=R_D}\, dz + 2\pi\int_0^{R_D} r\,[-pU_z + (-\boldsymbol{\tau}\cdot\mathbf{U})_z]|_{z=H}\, dr = \int_0^H \int_0^{R_D} 2\pi r\,(-\boldsymbol{\tau} : \nabla\mathbf{U})\, dr\, dz - 2\pi\int_0^{R_D} r\,[-pU_z + (-\boldsymbol{\tau}\cdot\mathbf{U})_z]|_{z=0}\, dr \quad (18)$$

Consequently,

$$\Delta p_{DE} = \frac{2\pi}{Q}\int_0^H \int_0^{R_D} r\,(-\boldsymbol{\tau} : \nabla\mathbf{U})\, dr\, dz - \frac{2\pi R_D}{Q}\int_0^H (-\boldsymbol{\tau}\cdot\mathbf{U})_r|_{r=R_D}\, dz - \frac{2\pi}{Q}\int_0^{R_D} r\,(-\boldsymbol{\tau}\cdot\mathbf{U})_z|_{z=H}\, dr + \frac{2\pi}{Q}\int_0^{R_D} r\,(-\boldsymbol{\tau}\cdot\mathbf{U})|_{z=0}\, dr \quad (19)$$

The components necessary to evaluate Equation (19) are

$$-\boldsymbol{\tau} : \nabla\mathbf{U} = k\,\{2\,[(\partial U_r/\partial r)^2 + (U_r/r)^2 + (\partial U_z/\partial z)^2] + (\partial U_\theta/\partial z)^2 + (\partial U_z/\partial r + \partial U_r/\partial z)^2\}^{(n+1)/2}$$

$$(-\boldsymbol{\tau}\cdot\mathbf{U})_r = k\,\dot\gamma^{\,n-1}\left[2U_r\frac{\partial U_r}{\partial r} + U_z\,(\partial U_z/\partial r + \partial U_r/\partial z)\right] \quad (20)$$

$$(-\boldsymbol{\tau}\cdot\mathbf{U})_z = k\,\dot\gamma^{\,n-1}\,[U_\theta\,(\partial U_\theta/\partial z) + 2U_z\,(\partial U_z/\partial z)]$$

$$\dot\gamma = \left(\frac{1}{2}\boldsymbol{\Delta}_{II} : \boldsymbol{\Delta}_{II}\right)^{1/2}$$

where

$$\boldsymbol{\Delta}_{II} = \nabla\mathbf{U} + (\nabla\mathbf{U})^T$$

It should be noted that

$$(-\boldsymbol{\tau}\cdot\mathbf{U})_r|_{r=R_D} = 2k\left(\dot\gamma^{\,n-1}\,U_r\frac{\partial U_r}{\partial r}\right)\Bigg|_{r=R_D}$$

$$(-\boldsymbol{\tau}\cdot\mathbf{U})_z|_{z=H} = 0$$

$$(-\boldsymbol{\tau}\cdot\mathbf{U})_z|_{z=0} = k\left(\dot\gamma^{\,n-1}\,U_\theta\frac{\partial U_\theta}{\partial z}\right)\Bigg|_{z=0}$$

Since analytical expressions are available for **U** [see Equation (16)], it is possible to evaluate numerically Equation (19) for any n desired. For $n = 1$, a Newtonian viscosity, the result is

$$\Delta p_{DE} = \frac{16}{\pi}\frac{kQ}{H^3}\left\{\frac{11}{64} + \frac{1}{5}(H/R_D)^2 + \frac{13}{70}(H/R_D)^4\right\} \quad (21)$$

For $n \neq 1$, other terms can become significant and must be calculated according to Equation (19). Δp_{DE} can be a significant contribution to the resistance to flow in the extruder. For the materials used in our extruder, the resistance in the die entrance was frequently greater than the total resistance to flow through the die.

REGION III: DIE FLOW PROPER

Boundary condition (15b) applies throughout the die, thus fully developed laminar power flow is assumed. Exit effects are neglected.

It is now possible to calculate the flow rate from the extruder. From Equation (5) the flow through the die is of the form

$$Q^n = \Theta\,\Delta p_T$$

where Δp_T is now

$$\Delta p_T = \Delta p_{NS} + \Delta p_E - \Delta p_{VS} - \Delta p_{DE} \quad (22)$$

The predicted flow through the die is

$$Q^n = \Theta\,\frac{\sum_{i=1} k_i\frac{m_i+3}{R}\int_{R_D}^{R}\bar\gamma^{\,m_i}\,dr + \Delta p_E}{1 + \Theta\frac{6}{\pi H^3}Q^{(1-n)}\int_{R_D}^{R}\frac{k\,\dot\gamma^{\,n-1}}{r}\,dr + \Theta\Omega} \quad (23)$$

where

$$\bar\gamma^2 = \frac{1}{H}\int_0^H \{2\,[(\partial V_r/\partial r)^2 + (V_r/r)^2] + (\partial V_\theta/\partial z)^2 + (\partial V_r/\partial z)^2\}\, dz$$

and

$$V_r = \frac{3Q}{\pi r H^3}\,z(z-H); \quad V_\theta = \frac{\omega r}{H}(H-z)$$

Typical components of Δp_E would be the external pres-

TABLE 1. RELATIVE RESISTANCE TO FLOW IN THE EXTRUDER FOR POLYACRYLAMIDE AT 28°C AND $\omega = 6.3\ s^{-1}$

H, cm	Resistance (dimensionless)		
	Die	Disk proper	Die entrance
0.050	1.00	5.00	1.25
0.075	1.00	1.97	0.71
0.100	1.00	0.97	0.53
0.150	1.00	0.32	0.41
0.200	1.00	0.15	0.37

TABLE 2. MATERIAL PROPERTIES

Polymer	Polyacrylamide American Cyanamid Co. Cyanamid P250	Polyisobutylene STP Corp. "STP Oil Treatment"	Polyethylene (from Fritz, 1971) Lupolen 1800H
Wt. %	5.0%	~18%	100%
Solvent	50-50 water glycerin by wt.	motor oil	none
Temperature	26°C	20°C	150°C
Density, g/cm³	1.16	0.92	0.92
Power law parameters, Eq. (1)			
k	17.28	110.	8.69×10^4
n	0.661	0.924	0.40
Normal force parameters, Eq. (3)			
k_1	140.	13.42	4.6×10^6
m_1	1.06	1.84	0.79
k_2	—	-4.9×10^{-3}	—
m_2	—	3.12	—

sure difference imposed on the extruder, hydrostatic pressure, and the centrifugal force on the material in the extruder. For stable operation $\Delta p_E \geqq 0$.

Equation (23) can be solved iteratively for Q. This is a particularly useful form, as a high trial value of Q used to evaluate the right side of Equation (23) will result in an underestimation of Q. Consequently, the true value of Q is bounded by one evaluation of Equation (23) and the true value can be determined with very few iterations. Equation (23) predicts Q to be small for small H, increasing rapidly to some maximum value as H increases, then slowly declines as H continues to increase. This is precisely the behavior observed experimentally (Maxwell and Scalora, 1959; Maxwell, 1970; Fritz, 1971). The influence of the various resistances to flow in Equation (23) are examined for a polyacrylamide solution (see Table 2) for various H with $\omega = 6.3$ s^{-1} in Table 1. Resistance to flow in the die has been assigned a value of 1. The resistance to flow in the disk proper and the die entrance are given relative to this value. For example the flow observed at $H = 0.075$ cm is $1./(1. + 1.97 + 0.71) = 0.272$ of the flow which would be observed if the resistance to flow in the disk proper and the die entrance could be neglected. These results are also shown graphically in Figure 2.

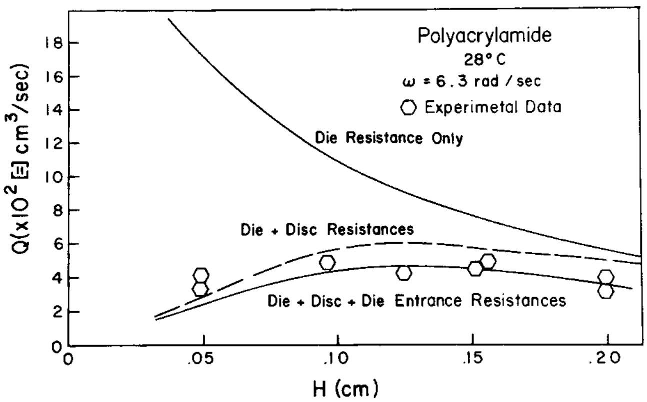

Fig. 2. The effect of the different resistances on the calculated flow rate.

EXPERIMENT

Several simple experiments were performed to test this analysis. A Rheometrics Mechanical Spectrometer (Macosko and Starita, 1971) was used to characterize the materials and also to drive the normal stress extruder.

A commercial polyisobutylene solution, STP oil additive, and polyacrylamide solution in water-glycerin were used. Their compositions and properties are summarized in Table 2. Shear stress data were collected in a cone and plate geometry and the normal force from total thrust in the parallel plate geometry. Data are plotted in Figures 3 and 4. Note that the rheology of these two solutions is considerably different. STP has a nearly Newtonian shear stress while the polyacrylamide is quite pseudoplastic. Their normal force functions are also different. STP appears to be a convenient viscoelastic material for experimenters; however, we have found some batch-to-batch variation.

The Mechanical Spectrometer could also function as a normal stress extruder by drilling a hole in the fixed plate of the parallel plate geometry. A die plate 7.2 cm in diameter was used with a die 0.245 cm in diameter and 0.482 cm long. The rotating plate was 5.0 cm in diameter. A 0.62 cm high dike was constructed around the die plate and filled with the polymer solutions. As material was extruded, it was periodically collected and weighed to obtain the flow rate. Results are presented as the points in Figures 5 to 7. The curves are from Equation (23).

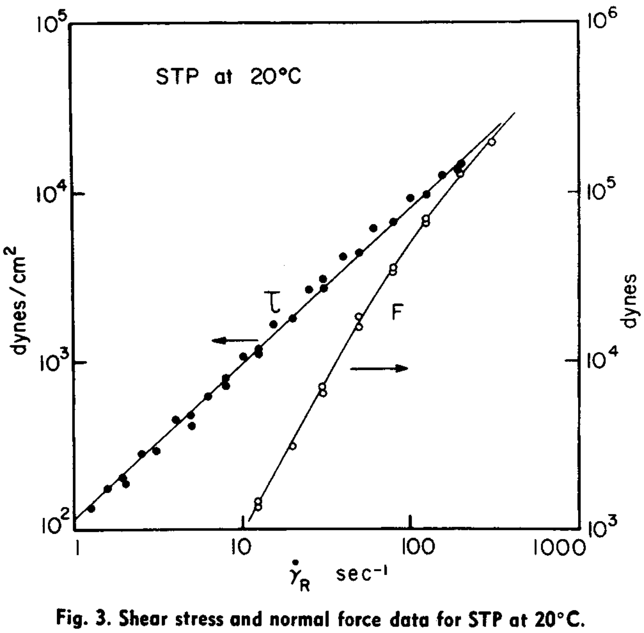

Fig. 3. Shear stress and normal force data for STP at 20°C.

DISCUSSION

Blyler (1966) and Maxwell (1970) observed roughly a linear relation between Q and ω. This is not in disagreement with our results in Figure 5. However, we find by Equation (23) that the relation will be more complex at small ω.

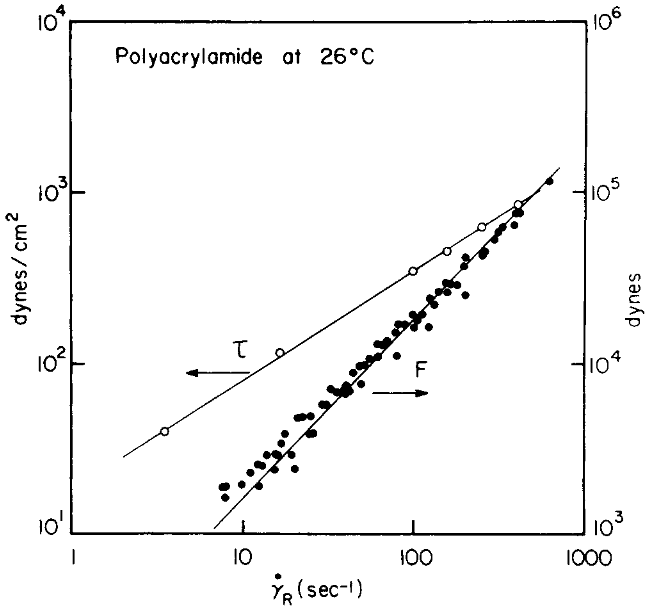

Fig. 4. Shear stress and normal force data for polyacrylamide at 26°C.

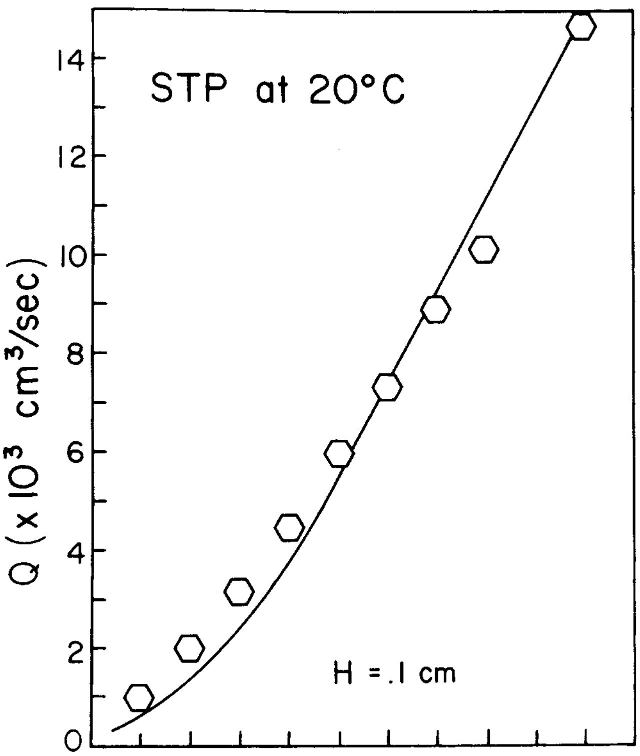

Fig. 5. Extrusion rate for STP at 20°C as a function of rotation rate ω at constant gap thickness ($H = 0.1$ cm).

Figures 6 and 7 show that there is an optimum gap for constant angular velocity. This was expected from Equation (23) and it is the point where the elastic pressure increase is balanced by viscous drag as H decreases, that is, where

$$\frac{\partial \Delta p_{NS}}{\partial H} = \frac{\partial(\Delta p_{VS} + \Delta p_{DE})}{\partial H}$$

An approximately constant optimum gap was observed for polymer melts by Maxwell (1959, 1970) and by Fritz (1971).

The data in Figures 6 and 7 are fit reasonably well by Equation (23). For the polyacrylamide agreement is within the experimental accuracy for $H > R_D$. For $H \lesssim R_D$ the pressure at the die entrance is really not uniform and the approximate analysis of the entrance region breaks down. This leads to an overestimation of resistance to flow in the entrance region. At $\omega = 10$ rad/s the polyacrylamide solution tended to climb out and over the back plate and is probably responsible for the poor fit of that data.

The STP shear and normal force characterizations were carried out at 20°C while the flow rates in Figure 6 were determined at 30°C. The temperature dependence of STP

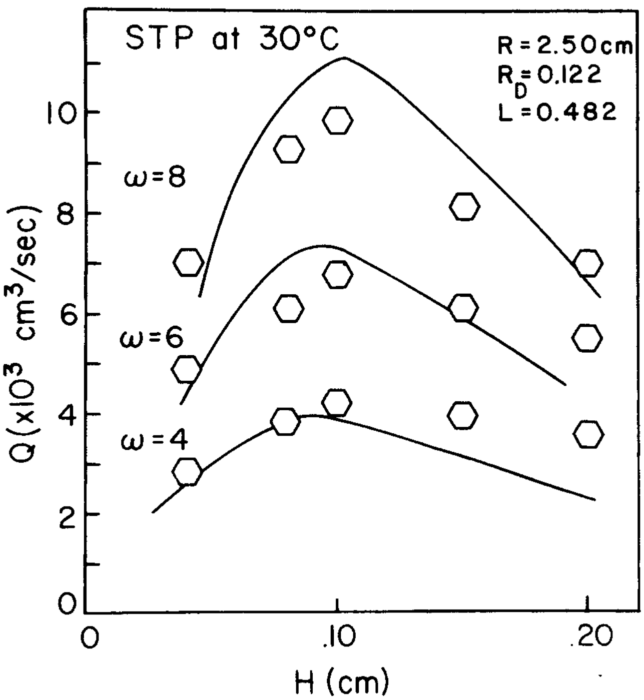

Fig. 6. Extrusion rate for STP at 30°C as a function of rotation rate ω and gap thickness H.

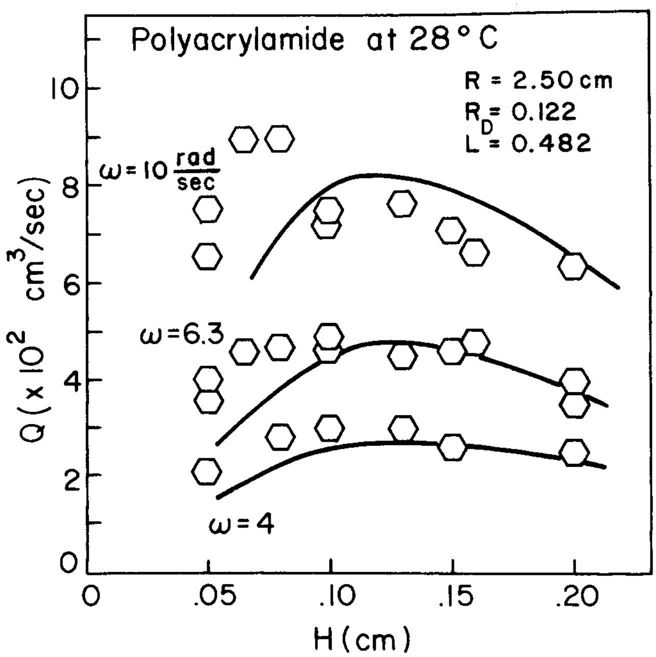

Fig. 7. Extrusion rate for polyacrylamide at 28°C as a function of rotation rate ω and gap thickness H.

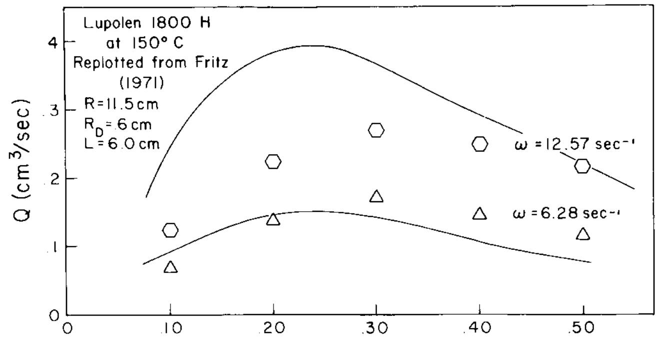

Fig. 8. Extrusion rate for Lupolen 1800 *H* entering at 150°C as a function of rotation rate ω and gap thickness *H*.

was found to be relatively small, less than 5% decrease in F_z, and less than 1% in τ from 20 to 25°C. This is in agreement with Tanner's (1973) survey of polyisobutylene data. Thus shear and normal force parameters were not adjusted since the changes would be within the accuracy inherent in the extrusion experiment.

Fritz (1971) reports flow rates of a branched polyethylene in a normal stress extruder. He provides rheological data shown in Table 2. His extruder dimensions and some results are shown in Figure 8. Note that the rheological properties and extruder dimensions are considerably different from those in Figures 6 and 7. Curves are again from Equation (23).

Due to the high viscosity of the polyethylene, shear heating is significant. At $H = 0.15$ cm Fritz reports measured temperatures near the periphery of the disk of up to 185°C for $\omega = 6.28$ rad/s and 250° for 12.57 rad/s. Thus the simple isothermal model used here should over predict the flow rates since it can't account for the decrease in the strongly temperature dependent normal force. Material properties for Figure 8 were evaluated at an average temperature observed for each ω. For $\omega = 6.28$ s^{-1}, the temperature was 173°C, for $\omega = 12.57$ s^{-1}, the temperature in the extruder was much higher for small H than for large H, hence the discrepancy of experimental and calculated results.

It appears that to model more viscous polymer melts the energy equation will need to be solved with temperature dependent viscous and elastic properties. Work is in progress in this direction.

NOTATION

F = normal force on parallel plate, dynes
H = gap thickness, cm
$\mathbf{I}$ = idemfactor tensor
k = power law viscosity, dyne s^n/cm^2
L = length of the die, cm
$\mathbf{N}$ = elastic normal stress tensor, dynes/cm²
n = exponent for the power law
$\mathbf{P}$ = total stress tensor, dynes/cm²
p = isotropic pressure, dynes/cm²
Q = flow rate, cm³/s
r = radial coordinate, cm
R = back plate radius, cm
S = surface of volume V
T = temperature, °Kelvin
$\mathbf{U}$ = velocity in the die entrance section, cm/s
$\mathbf{V}$ = velocity in the disk proper, cm/s
V = volume of the entrance region, bounded by $r = R_D$, $0 \leq z \leq H$
z = polar coordinate, cm

Greek Letters

α $= \dfrac{1+3n}{1+n}\dfrac{Q}{\pi R_D^2}$, cm/s
β $= \dfrac{3Q}{\pi R_D H^3}$, $cm^{-1}s^{-1}$
$\dot{\gamma}$ = shear rate, s^{-1}
$\mathbf{\Delta}$ = rate of strain tensor defined as $\nabla\mathbf{V} + (\nabla\mathbf{V})^T$, s^{-1}
Θ $= \left(\dfrac{\pi n}{1+3n}\right)^n \dfrac{R_D^{1+3n}}{2kL}$, cm^{2+3n} $dyne^{-1}$ s^{-n}
θ = polar coordinate, radians
ρ = density, g/cm³
Φ $= \dfrac{6Q}{\pi R_D^2 H^3}\dfrac{1+3n}{1+n}$, s^{-1} cm^{-2}
Ω = defined as

$$Q^{-(1+n)}\left(\int_0^{R_D} 2\pi \int_0^H (-\boldsymbol{\tau}):(\nabla\mathbf{U})r\,dz\,dr - \int_S \hat{\mathbf{n}}\cdot(-\boldsymbol{\tau})\cdot\mathbf{U}\,dS\right)$$

ω = angular velocity, radians/s

Subscripts

D = die
DE = die entrance
E = external
NS = normal stress
R = quantity evaluated at $r = R$
T = total
VS = viscous stress

Superscripts

— = averaged quantity $\overline{A} = \dfrac{1}{H}\int_0^H A\,dz$
T = transpose of a tensor

LITERATURE CITED

Blyler, L. L., Jr., "Analysis of Normal Stress Extrusion of Polymer Melts," Ph.D. thesis, Princeton University, N. J. (1966).

———., T. W. Huseby, and S. Matsuoka, paper presented at Conf. on Adv. Polymer Science and Materials, Princeton University, N. J. (1968).

Fritz, H. G., "Die theoretische und experimentelle Untersuchung eines Drehscheibenextruders, dessen Funktionsweise ausschliesslich auf dem Normalspannungseffekt nach Weissenberg beruht," Ph.D. thesis, Stuttgart Univ., Germany (1971).

Kocherov, V. L., Yu. L. Lukach, E. A. Sporyagin, and G. V. Vinogradov, "Flow of Polymer Melts in a Disc Type Extruder and in Rotational Devices of the 'Cone-Plate' and 'Plate-Plate' Type," *Polymer Eng. Sci.*, **13**, 194 (1973).

Macosko, C. W., and J. M. Starita, "A New Rotational Rheometer," *S.P.E. Tech. Papers*, **17**, 595 (1971); *S.P.E. J.* **27**, 38 (1971).

Maxwell, B., and A. J. Scalora, "The Elastic Melt Extruder—Works Without Screw," *Modern Plastics*, **37**, 107 (1959).

Maxwell, Bryce, "Scaling Up the Elastic Melt Extruder," *S.P.E. J.*, **26**, 48 (1970).

———., "The Application of Melt Elasticity to Polymer Processing," *Polymer Eng. Sci.*, **13**(9), 227 (1973).

Middleman, S., *The Flow of High Polymers*, pp. 54-57, Interscience, New York (1968).

Paul, D. R., C. E. Vinson, and C. E. Locke, "The Potential for Reuse of Plastics Recovered from Solid Wastes," *Polymer Eng. Sci.*, **12**, 157 (1972).

Starita, J. M., "Microstructure of Melt Blended Polymer Systems," *Trans. Soc. Rheol.*, **16**, 339 (1972).

Tanner, R. I., "A Correlation of Normal Stress Data for Polyisobutylene Solutions," *ibid.*, **17**, 365 (1973).

Manuscript received July 3, 1973; revision received August 23 and accepted August 24, 1973.